Electromagnetic characterisation of materials using complementary frequency selective surfaces

ELECTROMAGNETIC CHARACTERISATION OF MATERIALS USING COMPLEMENTARY FREQUENCY SELECTIVE SURFACES

ESA/ESTEC, NOORDWIJK, THE NETHERLANDS
10-13 SEPTEMBER 2013

Yiannis C. Vardaxoglou [*1], Chinwe C. Njoku [*2], William G. Whittow [*3]

[*] *School of Electronic, Electrical & Systems Engineering, Loughborough University, Loughborough, LE11 3TU, UK*
Email: {[1]eljcv, [2]elccn, [3]elwgw}@lboro.ac.uk

ABSTRACT

This paper explores the concept of using the resonant nature of complementary frequency selective surfaces (CFSS) placed in a waveguide to characterise the permittivity of homogenous dielectric materials. Electromagnetic simulations using the 3D FDTD software, Empire XCcel® have been used to characterise some of the properties of this CFSS-Waveguide technique and used in the extraction of the permittivity of these materials. The simulation setup, well-known extraction equations and their modified versions, along with the extracted results are presented in this paper.

1. INTRODUCTION

Several techniques have been developed over the years for the measurement of the dielectric properties of various homogenous substrate materials used in the increasingly diversified antenna systems world. The antenna substrate is a very important component of the antenna system and as such the better the accuracy of the measured dielectric properties of these materials, the better the antenna design. These dielectric characterisation techniques include the waveguide transmission/reflection approach [1], [2], [3], split-post dielectric resonators (SPDR) [4], [5] and microstrip line and ring resonators [6], [7], [8], [9], amongst others. Some of these methods are limited; for example, with the plane wave method – in which diffraction around the edges can reduce the accuracy of the results and the need to have a large enough sample in the far field of the source.

This paper extends the application of Complementary Frequency Selective Surfaces (CFSS), first introduced by Lockyer et al in order to create an array of frequency selective surfaces (FSS) with angular and polarisation stability [10], in determining the ε_r of various homogenous substrates. The CFSS as shown in Fig. 1 consists of two FSS structures – an array of dipoles/conductors and an array of apertures/slots, separated by a thin low loss dielectric material, in order to lower the resulting resonant frequency of the combined FSS's. The individual resonant frequencies of the arrays alone are at higher frequencies that when combined to form the CFSS. Some of the advantages of using this technique are the low insertion loss, the stability and high Q-factor of the passband which occur at frequencies lower than those of the individual FSS structures. These properties of the CFSS make it suitable for permittivity measurements of dielectric substrates.

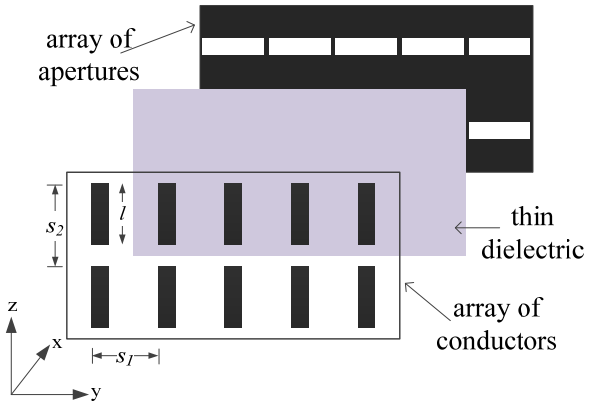

Figure 1. Exploded view of Complementary frequency selective surfaces (CFSS)

In Section 2, the CFSS-Waveguide measurement method is outlined while Section 3 presents the simulated results of parametric studies carried out on the CFSS with the MUT in order to properly understand the operation of the CFSS-Waveguide measurement technique, with respect to the geometric and dielectric properties of the MUT. In Section 4, the extraction technique and equations are presented while Section 5 gives the results from simulations of various materials of different permittivities, and compared with the known simulated values. Finally the conclusions are given in Section 6 along with recommended future work.

2. METHOD OUTLINE

The CFSS is loosely based on the Babinet's principle, which states that: "when the field behind a screen with an opening is added to the field of a complementary structure, the sum is equal to the field when there is no

screen" [11]. The array of dipoles and slots are complementary, centred and at 90° to each other.

A suitable CFSS structure is placed within an X-band waveguide and simulated using the FDTD simulation tool, Empire XCcel® as shown in Fig. 2. The length of the conductors and apertures are represented by l, while the unit cell size is $s_1 \times s_2$ as in Fig. 1. In ensuring the dimensions of the elements of these arrays are identical and bringing them in very close proximity, the "transmission responses produced by the two layers interact" [10], creating a narrow passband at lower frequencies than that of the individual arrays as shown in Figure 3. This passband is highly stable with angle/frequency.

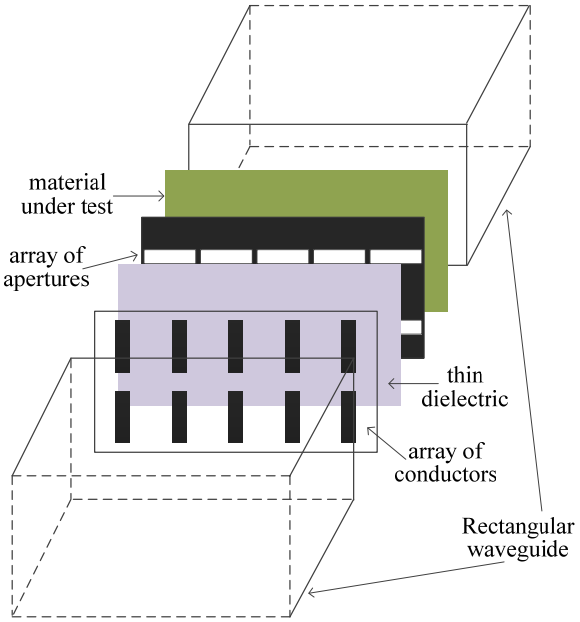

Figure 2. CFSS-Waveguide simulation arrangement

Once the dimensions of the elements have been selected such that the CFSS structure resonates at the desired frequency, the unknown dielectric material (MUT) is placed behind it. The resonant frequency now decreases as the structure has more dielectric loading. Thus by using the thickness of the material and these resonant frequencies, the permittivity of the material can be determined. By comparing this shift in resonant frequency for the unknown sample to that of a known sample, the ε_r of the MUT can be determined [12], without the need for phase information.

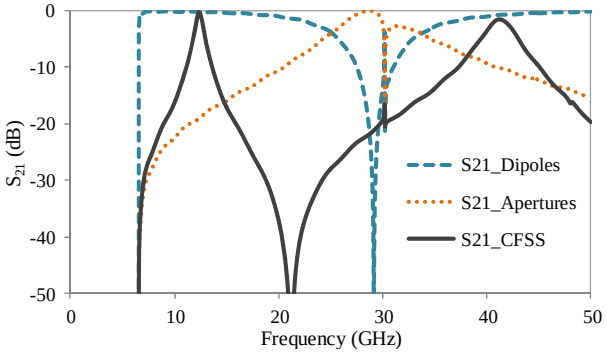

Figure 3. Transmission responses of the CFSS, the dipole array and the aperture array

Placing the CFSS in a waveguide allows the control of the measurement environment and helps to minimise errors. Once the waveguide has been properly calibrated, there is no need to know the position of the MUT as phase is not required.

3. PARAMETRIC STUDIES

In order to further understand how the CFSS works on its own and with a MUT, a number of parametric studies on the some of the parameters contributing to the resonance of the CFSS structure. These parameters include the thickness, permittivity and loss tangent of the dielectric separating the two FSS's, the lengths and periodicity of the apertures and conductors, the air gaps between the CFSS and the MUT, the thickness of the MUT samples, and the dielectric and/or magnetic properties of the MUT. An initial study on some of the properties of the CFSS structure itself has been presented in [13]. Common simulation data: $s_1 \times s_2 =$ 4.57 mm × 5.08 mm, length of slots and dipoles, $l =$ 4.32 mm, dielectric properties of in-between dielectric, $\varepsilon_{id} =$ 2.50, $\tan\delta = 0.0019$, thickness of in-between dielectric, d_{id} =70 µm, X-band waveguide dimensions: 22.86 mm by 10.16 mm (frequency range: 8.2 – 12.4 GHz), $\varepsilon_{MUT} =$ 3.5, $\tan\delta_{MUT} = 0.0018$, thickness of MUT, $d_{MUT} = 0.5$ mm.

This section looks at those parameters that include the presence of the MUT such as the properties of the MUT and the air gaps between the CFSS and the MUT.

3.1 Thickness of the MUT

Fig. 4 shows how the variation of the MUT thickness affects the performance of the CFSS. As the thickness of the MUT increases, the resonant frequency, f_r and the Q-factor reduces while the insertion loss increases

slightly. The reduction in f_r between consecutive thicknesses is not significant as the MUT gets thicker. This reduction has also been reported in published papers [14], [15]. However, to ensure a good-enough coupling of the fields from the CFSS to the MUT, the MUT should not be too thick. From these results, the recommended thickness should be in the 1.5 mm region.

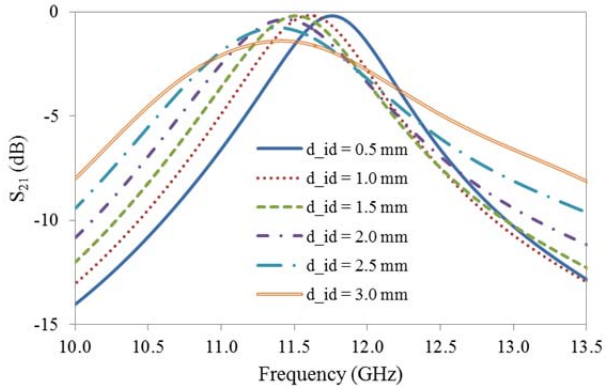

Figure 4. S_{21} variation of MUT thickness with frequency

Although the extraction equations (see Eqs. 1-2) do not include the thickness difference between the test and reference substrates, the equations can be modified as in [16] to include any differences in thicknesses.

3.2 Permittivity of the MUT

As the aim of the CFSS-Waveguide technique is to characterise dielectric substrates, Fig. 5 shows the variation of f_r with change in the permittivity of the MUT, ε_{MUT}. As this permittivity increases, the resonant frequency reduces and the insertion loss increases while the Q-factor increases. This is as expected from general microwave theory as the dielectric loading on the CFSS increases. In this study, the loss tangent was kept constant at 0.0018.

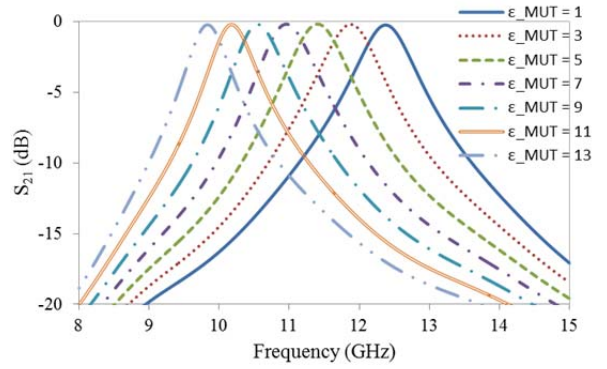

Figure 5. S_{21} variation of MUT permittivity with frequency

Worthy of note in Fig. 4 is the stability of the insertion loss and the Q-factor in the frequency response of the CFSS as the permittivity increases.

3.3 Air gaps between CFSS and MUT

The study of the effect of the air gaps between the CFSS and the MUT is crucial as during measurements, it would be near impossible to ensure 100% surface contact of the CFSS with the MUT once placed in the waveguide sample holder such as a waveguide offset. Fig. 5 shows the effect of the size of these air gaps, d_a. As the air gaps increase, the resonant frequency increases. As shown in Fig. 6, the S_{21} frequency responses tend to cluster around the same frequency region, that is, the difference in f_r between consecutive air-gap thicknesses is not significant. This increase is expected as the effective dielectric loading seen by the CFSS is reduced by the presence of the air gaps.

It is also important for the sample to cover the whole waveguide aperture, otherwise a difference in the resonant frequency is obtained [4].

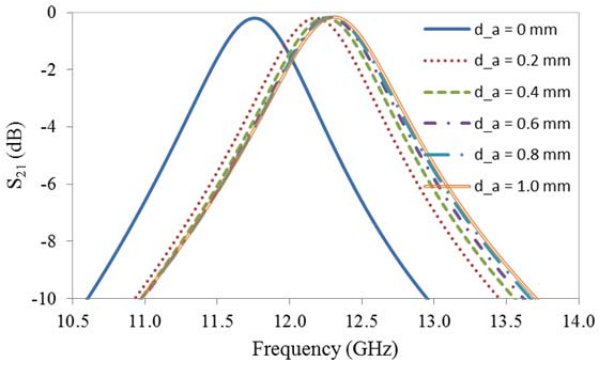

Figure 6. S_{21} variation of air gap between CFSS and MUT with frequency

4. EXTRACTION TECHNIQUE

As stated earlier, the extraction process is similar to the SPDR and the equations for extracting the ε_r and the loss tangent, $\tan\delta$ of the MUT are given as [12]:

$$\varepsilon_r = \frac{\Delta f_r}{\Delta f_{r0}}(\varepsilon_{r0} - 1) + 1 \quad (1)$$

$$\tan\delta = \frac{\varepsilon_{r0}-1}{\varepsilon_{r0}} \cdot \frac{f_r}{\Delta f_r}\left(\frac{1}{Q} - \frac{1}{Q_0}\right) + \tan\delta_0 \quad (2)$$

where $(\varepsilon_{r0}, \tan\delta_0)$ are the permittivity and loss tangent of a reference sample, $(\Delta f_r, \Delta f_{r0})$ are the changes in resonant frequencies of the CFSS from

its unloaded state with the MUT and the reference sample respectively, and (Q, Q_0) are the Q-factors of the CFSS with and without the MUT. These equations are based on the perturbation theory of dielectric objects in a cavity [17], [18], [19]. By using this theory and assuming equal volumes of the test and reference samples, Eqs. 1-2 can be modified to:

$$\varepsilon_r = \frac{\Delta f_r}{\Delta f_{r0}} \cdot \frac{f_{r0}}{f_r}(\varepsilon_{r0} - 1) + 1 \quad (3)$$

$$\tan\delta = \frac{\varepsilon_r}{\varepsilon_{r0}} \tan\delta_0 \frac{\Delta Q}{\Delta Q_0} \frac{Q_0}{Q} \quad (4)$$

Eqs. 3-4 were obtained by using a finding the ratio between the unknown permittivity, ε_r and the known permittivity, ε_{r0}, using the perturbation equations in [16]. Eq. 1 is also similar to that used in the SPDR in [16] which also gives a more complex equation for the extraction of the loss tangent using energy filling factors [5] which has not been considered in this paper. Reference [16] can also be used to take into account cases where the thickness of the reference substrate and the MUT are different, modifying Eq. 1 by including a thickness ratio to the multiplying factors.

It should be noted that the permittivity of the reference sample, ε_{r0} cannot be 1 as that would always make $\varepsilon_r = 1$, and $\tan\delta = \tan\delta_0$.

5. SIMULATED RESULTS

In this section, Eqs. 1-2 were used to determine the ε_r of the samples simulated in Section 3.2 and the results are shown in Tab. 1. Common data used: $d_{MUT} = 0.5$ mm, $\tan\delta_{MUT} = 0.0018$ (same simulation data as in Section 3 was used here). ε_{eff} represents the extracted permittivity value using Eq. 1. The reference sample used has the same thickness as the MUT; its permittivity, $\varepsilon_{ref} = 4.5$, $\tan\delta_{ref} = 0.0037$, and its simulated resonant frequency, $f_{r0} = 11.53$ GHz, S_{21} = -0.23 dB and Q = 13.74. The resonant frequency of the CFSS alone, $f_0 = 12.37$ GHz, S_{21} = -0.24 dB and Q = 15.16.

Table 1: Simulated and extracted results

ε_{MUT}	f_r (GHz)	S_{21} (dB)	Q	ε_{eff}	ε_{eff2}	$\tan\delta_{eff2}$ (×10^{-4})
1	12.38	-0.25	15.12	1.02	1.01	4.22
3	11.88	-0.21	14.33	3.05	2.99	0.31
5	11.41	-0.19	13.69	5.00	5.04	0.34
7	10.96	-0.19	13.92	6.84	7.14	0.20
9	10.55	-0.21	14.83	8.53	9.22	3.89
11	10.18	-0.22	15.69	10.06	11.26	4.83
13	9.84	-0.23	16.18	11.48	13.27	7.65

ε_{eff} values were obtained using Eq. 1 while ε_{eff2} values were obtained using Eq. 3. As shown in Tab. 1, most of the extracted ε_{eff} permittivities are within 10% of the simulated values while the ε_{eff2} permittivities are within 2.5% of the simulated values. This implies that Eq. 3 may be more suitable than Eq. 1 for the extraction process.

The deviation from the known simulated values using Eq. 1 increases as the difference of these known values from that of the reference sample increases. This suggests that data from more reference samples than that of one known sample maybe required as done in the SPDR cases [5], [16]. It may also be more accurate to choose a reference sample whose permittivity is in the neighbourhood of that of the MUT. If the values for $\varepsilon_{MUT} = 7$ are used to determine the ε_{eff} for $\varepsilon_{MUT} = 9$, a closer value of 8.74 is obtained.

The loss tangent values extracted using Eq. 4, were not close to the known simulated values. Therefore, further investigation is needed in order to properly extract accurate loss tangent values, even though the values shown in Tab. 1 are very low. Eq. 2 was not used here as it gives rather high and/or negative values when used to compute the values of the loss tangents. However, as an initial investigation, the extracted ε_{eff} and $\tan\delta_{eff}$ results are quite promising.

6. CONCLUSIONS

This paper has introduced the concept of using a CFSS in a waveguide to measure the dielectric properties of various homogenous dielectric materials. Simulated results of parametric studies have been presented along with extracted results of different materials. Further work will be done on increasing the number of reference samples used, with different thicknesses and permittivities, in order to obtain better accuracy in the extracted results. Further research is needed on combining Eqs. 1 and 3, in the extraction of ε_{eff}, to get a more robust equation, and also on accurately extracting the loss tangents of the MUT's.

7. REFERENCES

1. Weir, W.B. (1974). Automatic measurement of complex dielectric constant and permeability at microwave frequencies. *Proc. of the IEEE*. **62**(1), 33-36.

2. Nicolson, A.M. & Ross, G.F. (1970). Measurement of the intrinsic properties of materials by time-domain techniques. *IEEE Transactions on Instrumentation and Measurement*. **19**(4), 377-382.

3. Boughriet, A.-H., Legrand, C. & Chapoton, A. (1997). Noniterative stable transmission/reflection method for low-loss material complex permittivity determination. *IEEE Trans. on Microwave Theory and Technique*. **45**(1), 52-57.

4. Krupka, J., Derzakowski, K. & Hartnett, J.G. (2009). Measurements of the complex permittivity and the complex permeability of low and medium loss isotropic and uniaxially anisotropic metamaterials at microwave frequencies. *Measurement Science and Technology*. **20**(10), 1-5.

5. Krupka, J., Gregory, A.P., Rochard, O.C., Clarke, R.N., Riddle, B. & Baker-Jarvis, J. (2001). Uncertainty of complex permittivity measurements by split-post dielectric resonator technique. *Journal of the European Ceramic Society*. **21**(15), 2673-2676.

6. Bernard, P.A. & Gautray, J.M. (1991). Measurement of dielectric constant using a microstrip ring resonator. *IEEE Transactions on Microwave Theory and Techniques*. **39**(3), 592-595.

7. Yamashita, E. & Mittra, R. (1968). Variational method for the analysis of microstrip lines. *IEEE Transactions on Microwave Theory and Technique.* **MTT-16**(4), 251-256.

8. Waldron, I., Makarov, S.N., Biederman, S. & Ludwig, R. (2006). Suspended ring resonator for dielectric constant measurement of foams. *IEEE Microwave and Wireless Components Letters*. **16**(9), 496-498.

9. Heinola, J.-M., Silventoinen, P., Latti, K., Kettunen, M. & Strom, J.-P. (2004). Determination of dielectric constant and dissipation factor of a printed circuit board material using a microstrip ring resonator structure. In *Proc. 15th International Conference on Microwaves, Radar and Wireless Communications*, Warszawa, Poland, pp202-205.

10. Lockyer, D.S., Vardaxoglou, J.C. & Simpkin, R.A. (2000). Complementary frequency selective surfaces. *IEE Proc. - Microwaves, Antennas and Propagation*. **147**(6), 501-507.

11. Balanis, C.A. (1997). *Antenna theory: analysis and design*. 3rd ed., Wiley Publishers, Chichester, USA, pp697-701.

12. Nishikawa, T., Wakino, K., Tanaka, H. & Ishikawa, Y. (1988). Precise measurement method for complex permittivity of microwave dielectric substrate. In *Proc. Conference on Precise Electromag. Meas.*, Ibaraki, Japan, pp155-156.

13. Njoku, C.C., Vardaxoglou, Y.C. & Whittow, W.G. (2013). Complementary frequency selective surfaces in a waveguide simulator. In *Proc. 7th European Conference on Antennas and Propagation*, Gothenburg, Sweden, pp2420-2422.

14. Callaghan, P., Parker, E.A. & Langley, R.J. (1991). Influence of supporting dielectric layers on the transmission properties of frequency selective surfaces. *IEE Proc. H - Microwaves, Antennas and Propagation*. **138**(5), 448-454.

15. Costa, F., Monorchio, A. & Manara, G. (2009). An equivalent circuit model of frequency selective surfaces embedded within dielectric layers. In *Proc. IEEE Antennas and Prop. Soc. Int.l Symp.*, Charleston, USA, pp1-4.

16. Krupka, J., Geyer, R.G., Baker-Jarvis, J. & Ceremuga, J. (1996). Measurements of the complex permittivity of microwave circuit board substrates using split dielectric resonator and reentrant cavity techniques. In *Proc. 7th Int.l Conf. on Dielectric Materials, Measurements and Applications*, Bath, UK, pp21-24.

17. Pozar, D.M. (2005). *Microwave Engineering*. 3rd ed., Wiley Publishers, India, pp298-307.

18. Matthew, K.T. (2005). Perturbation Theory. *Encyclopedia of RF and Microwave Engineering*. Wiley Online Library.

19. Vyas, A.D., Rana, V.A., Gadani, D.H. & Prajapati, A.N. (2008). Cavity perturbation technique for complex permittivity measurement of dielectric materials at X-band microwave frequency. In *Proc. International Conference on Recent Advances in Microwave Theory and Applications*, Jaipur, India, pp836-838.